Surgical Endoscopy (2023) 37:6197–6207
https://doi.org/10.1007/s00464-023-10105-x

Side-to-side duodeno-ileal magnetic compression anastomosis: design and feasibility of a novel device in a porcine model

Michel Gagner[1] · Todd Krinke[2] · Maxime Lapointe-Gagner[1] · J. N. Buchwald[3]

Received: 28 February 2023 / Accepted: 23 April 2023 / Published online: 11 May 2023

Abstract

Background Minimally invasive metabolic/bariatric surgery (MBS) may be further advanced by magnetic compression anastomosis (MCA) technology. The study aimed to develop a magnet sized to create a patent duodeno-ileostomy (DI) and verify its effectiveness in a porcine model.

Methods Developmental study phase: magnets with 4 different flange-offset dimensions were tested to identify a design that would successfully form a compression anastomosis. Verification phase: evaluation of the selected design's efficacy. In each 6-week phase (4 pigs/phase), one magnet was inserted laparoscopically in the jejunum, one placed gastroscopically in the duodenum. Magnets were aligned, gradually fused, formed an anastomosis, and then detached and were expelled. At necropsy, MCA sites and sutured enterotomy sites were collected and compared.

Results Developmental phase: the linear BC42 magnet with a 2.3-mm flange offset design was selected. Verification phase: in 4 swine magnets were mated at the target location, confirmed radiographically. Mean time to magnet detachment 16.0 days (12–22), to expulsion 24.5 days (17–33). MCA was achieved in all animals at time of sacrifice. Animals gained a mean 9.5 kg (3.9–11.8). Specimens revealed patent anastomoses of ≥ 20 mm with smooth mucosa and minimal inflammation and fibrosis compared to sutured enterotomies. One pig underwent corrective surgery for a mesenteric hernia without sequelae.

Conclusion In a large-animal model, gross and histopathologic examination confirmed that the linear MCA device created a patent, well-vascularized, duodeno-ileal anastomosis. The novel MCA device may be appropriate for use in human MBS procedures.

Keywords Magnetic compression anastomosis · MCA · Metabolic/bariatric surgery · MBS · Bariatric surgery · Duodeno-ileostomy

Metabolic/bariatric surgery (MBS) is the most effective and durable treatment for obesity with or without type 2 diabetes (T2D) [1]. Although minimally invasive laparoscopic and endoluminal techniques have made MBS markedly more acceptable to patients [2], further advances in safety, speed, and reduced costs may be possible by performing gastrointestinal (GI) anastomoses with magnetic compression rather than suturing and stapling.

✉ Michel Gagner
gagner.michel@cliniquemichelgagner.com

[1] Department of Surgery, Westmount Square Surgical Center, 1 Westmount Square, Suite 801, Westmount, QC H3Z2P9, Canada

[2] GT Metabolic Solutions, San Jose, CA, USA

[3] Division of Scientific Research Writing, Medwrite, Maiden Rock, WI, USA

Compression anastomosis (CA) devices have been employed for nearly two centuries, since Denan in 1826 introduced an end-to-end CA using two apposed metallic rings in canine intestine [3]. In 1892, Murphy invented a spring-loaded 'button' with two nickel-plated brass pieces that formed a rapid CA in GI tissue [4]; the Mayo brothers refined and popularized this device for colon reconstruction [5]. From the late twentieth century on, studies of CA were pursued in animal models [6–8], and in human trials evaluating ring- and memory-shaped devices for intestinal repair and treatment of inflammatory, obstructive, and diverticular diseases [9–17]. The first CA performed in clinical MBS incorporated a biodegradable version of the Murphy button in the duodeno-ileostomy (DI) of a duodenal switch [18].

While non-magnetic compression devices effectively form anastomoses, they require fixation with staples or sutures that remain in the body risking tissue damage

requiring reoperation [19, 20]. MCA technologies largely obviate retained foreign materials in the GI tract. A variety of MCA designs have been evaluated preclinically [21–28], some of which have progressed to clinical studies, including those primarily used to relieve intestinal obstruction (the 'magnamosis' device [29], and the samarium-cobalt magnet [30]); to palliate gastric outlet obstruction (the endoscopic gastroenteric anastomosis with magnets [EGAM] technology [31]); and to achieve MBS treatment objectives (self-assembling magnets [SAM] [32]). As yet, no MCA technology has been commercialized.

A new linear magnetic compression anastomosis device (MCAD) developed by our team forms a patent intestinal anastomosis over 7–21 days and is expelled naturally. The 'delayed anastomosis technology' (DAT) may reduce the risks of bleeding, leak, stricture, infection, and ulceration associated with conventional anastomosis creation [33]. This large-animal study aimed to determine MCAD dimensions capable of creating a patent side-to-side duodeno-ileal anastomosis and verify the safety and effectiveness of the device for use in a human DI procedure.

Methods

Study design

A two-part prospective preclinical study was undertaken in a porcine model, first, to evaluate magnet prototypes of varying sizes to determine dimensions suited to create a patent MCA in the small intestine, and second, to confirm the chosen design's safety and effectiveness. As the morphologic distinction between the jejunum and ileum is unclear in swine [34], the study procedure can be classified as a duodeno-enteral anastomosis, used synonymously with duodeno-ileostomy/DI herein in anticipation of its application in humans.

Ethics

The protocol was reviewed and approved by the animal testing facility's Institutional Animal Care and Use Committee (IACUC) to ensure compliance with the Canadian Council on Animal.

Care regulations. All animal enclosures met the standards of the National Academies of Science Guide for the Care and Use of Laboratory Animals [35]. *Written consent was not required for an animal study.*

Animal model

Young, 40–60-kg domestic Landrace-Yorkshire female farm pigs (Triporc, Inc., Sainte-Élisabeth, Canada) were selected as the test subjects as their intestinal anatomy and physiology are closest to that of humans, and provide an appropriate model for MBS.

Facility and feeding

The testing facility was a professional animal laboratory (#3139-609N) monitored daily by a trained veterinary team. Swine were individually housed in temperature- and humidity-controlled enclosures that were cleaned and washed daily. Each was installed with a standard magnet in its base to retain the surgical magnets for study when excreted from the swine. Animals were fed thrice daily with a certified contaminant-free powdered diet (Shur Gain, Trouw Nutrition, Puslinch, Ontario, CA) mixed with water or meal supplement (Ensure, Abbott Nutrition, Dayton, OH). The liquid diet was withheld 12 h prior to a procedure. After magnet expulsion, the diet was given in solid form. Tap water with no contaminants was provided ad libitum.

Testing

Selection of magnet size

Magnets engineered by our team used in this study for size selection, and for verification of safety and effectiveness, were under development between 2007 and 2019 (U.S. Patent #US-9801635-B2). Testing involved MCAD insertion into the porcine small intestine at a placement site approximating the location of a DI in humans. Each MCAD comprised a linear-shaped BC42 neodymium magnet (KJ Magnetics, Pipersville, PA) with a perimeter flange and titanium casing. Magnets needed to be sufficiently small that, when mated to form an anastomosis, they could detach from the anastomosis site and pass through the lumen of the small intestine. Each magnet was identical in dimensions (0.75″ length × 0.25″ width × 0.125″ thickness) and was magnetized along the axis of thickness (i.e., 0.125″). The single device variation under evaluation in this developmental phase was flange-offset height. An MCAD with a unique flange-offset height was inserted in each swine, i.e., (1) no flange, (2) 1.5-mm flange, (3) 3.0-mm flange, and (4) 4.5-mm flange. In this phase, 4 swine were included (with a fifth reserved as a potential replacement).

Verification of magnet safety and effectiveness

Based on size testing, the final flange-offset height was chosen for further evaluation. The selected MCAD was inserted gastroscopically or laparoscopically in the small intestine of a separate set of 4 swine (tagged #s W6-01, W6-02, W6-03, W6-04) to verify its safety and effectiveness in creating a patent DI.

Procedure

Prior to surgery, carprofen (Rimadyl; Parsippany, NJ) and buprenorphine HCl IM (Vetergesic; Whitby, ON, CA) were administered for pain prevention, and cefazolin for antibiotic coverage. Animals were anesthetized (with ketamine, azaperone, and atropine) and placed in dorsal recumbent position, intubated, and supported with mechanical ventilation. Isoflurane in oxygen was given to maintain a surgical plane of anesthesia. Bupivacaine was infiltrated prior to incision at the midline site. Intravenous fluid therapy was maintained throughout the procedure.

Abdominal access was established by midline laparotomy. The target anastomosis site was marked with a suture approximately 250 cm distal to the duodeno-jejunal flexure (corresponding to the ligament of Treitz in humans). A side-to-side small-intestinal anastomosis [36, 37] was created in which the distal magnet was inserted in the lower small intestine via enterotomy. The proximal magnet was placed gastroscopically into the duodenum, but if unsuccessful, a distal duodenostomy was performed (Fig. 1). The distal magnet was advanced through the lumen and placed at the target anastomosis site with a minimally invasive positioning tool (Fig. 2). The distal magnet was raised into alignment to pair with the proximal magnet. The enterotomy incision was closed with absorbable monofilament suture, and the laparotomy incision was closed in layers with absorbable monofilament suture with antibiotic ointment applied to the wound. A postoperative radiograph in AP view was taken to serve as a baseline image of magnet location for comparison with position-tracking radiographs once mated magnets detached from the anastomosis and started to move through the bowel. To reduce acid production, omeprazole (AstraZeneca, Wilmington, DE) 40 mg/pig, PO, BID mixed with food or another appropriate carrier was given daily starting postoperative day (POD) 1 until MCAD dislodgment. Polyethylene glycol (40 mL powder mixed in the food, BID) was given daily as a laxative until magnets passed per anus.

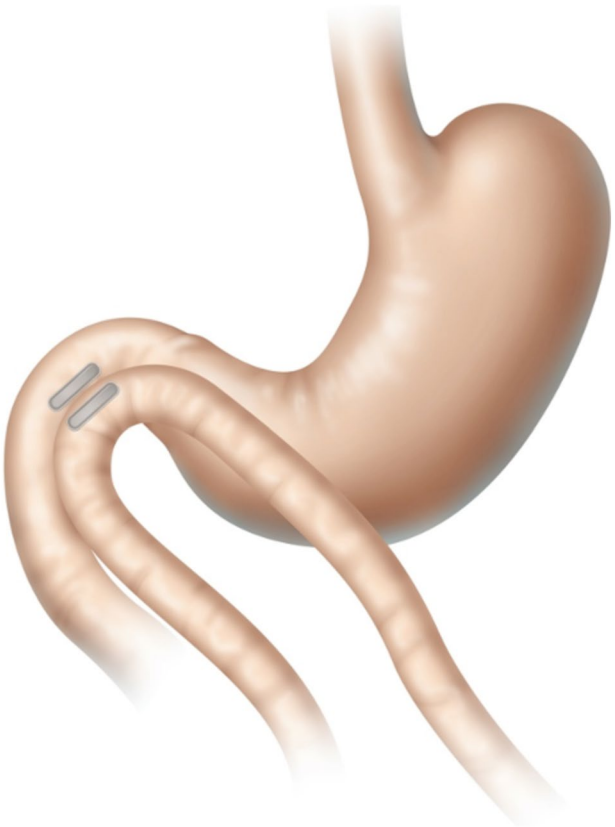

Fig. 1 Duodeno-ileal compression anastomosis by pairing of two linear magnets. The proximal magnet is positioned in the duodenum by gastroscopy and the distal magnet in the ileum by laparoscopy. After inter-magnet tissue compression and necrosis, the united magnets are expelled naturally

Recovery

During postoperative recovery in their enclosures, animals received carprofen 4 mg/kg, SC.or 3-5 mg/kg, PO, on POD 1 and 2 for pain relief. Movement of paired magnets away from the anastomosis was tracked radiographically (Siemens Artis Z Eco Fluor Fluoroscope, Munich, DE) under light anesthesia with propofol and isoflurane or isoflurane alone. Feces were evaluated at least twice daily to note magnet elimination. Body weight was measured twice weekly.

Euthanasia and necropsy

Animals were euthanized at the 6-week mark (42 ± 4 days). Final gastroscopy was performed (Evis EXERA II, Olympus, Center Valley, PA) and photographs taken of the anastomosis and enterotomy sites and of adjacent intraluminal locations to evaluate inflammation, wound healing, and anastomotic patency. Samples of the anastomosis and

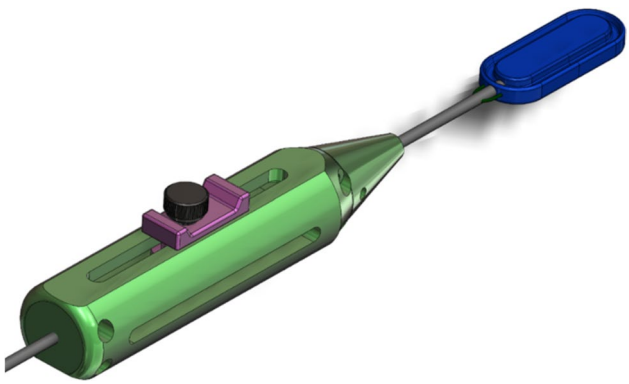

Fig. 2 Small-intestinal magnetic compression anastomosis delivery system

enterotomy sites were obtained and processed by immersion in neutral buffered formalin (NBF). A longitudinal section of the anastomosis site (including duodenum and ileum) and of the enterotomy site was embedded in paraffin, sectioned (to approximately 5 µm in thickness), slide mounted, and stained with hematoxylin and eosin (H&E). The duodenum was marked with black ink at histology trimming.

Macroscopic and histologic evaluation

Both anastomosis and enterotomy sites were examined macroscopically and histologically along multiple parameters to compare their healing response and the presence of inflammation, infection, or dehiscence at the sites of tissue apposition.

Results

Magnet development

At the time of procedure, the 4 swine were 4.2–4.7 months of age, and 43–47 kg. The 4 magnets of varying flange-offset height were inserted successfully in the swine and formed a DI anastomosis. One pig developed an internal hernia that resulted in death on postoperative day (POD) 4, which was determined to be unrelated to the magnets. The reserved fifth pig served as a replacement and underwent the same procedure and follow-up. The magnets were well tolerated postoperatively and, in each pig, a mated magnet pair was released into the intestinal lumen from the anastomotic site at a mean of 12.5 days (range 10–14) post procedure; anal expulsion occurred at a mean of 23.7 days (13–34).

The animals were euthanized at 6 weeks (42 ± 4 days). All swine had patent anastomoses and had gained a mean 13.7 kg (10.3–16.6) relative to baseline. On gross and microscopic evaluation, a good healing response was seen characterized by low levels of inflammation and tissue disruption. A moderate incidence of abdominal adhesions was observed interpreted as procedural in origin, unrelated to the magnetic anastomosis device or to sutures. Based on these findings, a BC42 magnet with 2.3-mm flange offset height was chosen for confirmatory testing.

Verification

To verify the effectiveness of the MCAD, on January 17th and 24th, 4 female swine (5.5–5.7 months old) of normal-weight (53.8–59.1 kg) underwent a side-to-side magnetic compression DI using MCADs of uniform dimensions comparable to those to be used in upcoming clinical studies. All 4 proximal magnets were placed gastroscopically; 3 distal magnets were positioned laparoscopically, and the fourth by laparotomy. There were no operative complications. At a mean of 16 days (12–22), the paired magnets were released from the anastomotic site into the intestinal lumen; expulsion occurred at a mean of 24.5 days (17–33) (Fig. 3).

Animals were closely monitored for infection, fever, abnormal mentation, low appetite or anorexia, vomiting, and abnormal posture. On POD 3, the first swine showed clinical signs of inflammation and dehydration and underwent exploratory and corrective surgery of a mesenteric hernia without further intervention.

At 6-week follow-up, as expected for growing swine, a mean of 9.5 kg (3.9–11.8) had been gained relative to baseline except for swine #W6-01, who lost weight post procedure but began gaining weight on day 15 (Table 1). Indicative of the intended weight loss following MBS, all pigs gained less weight in comparison to those of similar age, breed, and housing conditions but naïve to the study feeding regimen, surgery, recurrent fasting, and anesthesia for radiography.

The animals were euthanized on POD 39. Each had a patent anastomosis through which the gastroscope passed readily; no ulceration, inflammation, infection, or dehiscence was noted at any of the anastomoses (Fig. 4). On gross examination, the serosal aspect of the anastomosis and enterotomy site in all animals appeared healed (Fig. 5). Minor abdominal adhesions noted in 2 animals were similar to those typically observed in humans following abdominal surgery and were not attributed to magnetic anastomosis formation.

Microscopic evaluation compared the anastomoses created by magnetic compression to that made by the foreign bodies of sutures retained in the jejunal enterotomies. In each anastomosis, a good healing response was observed with lower levels of inflammation, fibrosis, and mesothelial hyperplasia and better serosal neovascularization than in the sutured jejunal enterotomies. No infiltration by plasma cells, macrophages or multinucleated giant cells in the anastomoses was noted, nor any necrosis, smooth muscle cell loss, hemorrhage, mineralization, injury, or fibrin accumulation (Fig. 6).

Relative to microscopic review of anastomosis samples, the 3 available jejunal enterotomy samples suggested that suture implantation was associated with higher levels of granulomatous inflammatory infiltrate with occasional tertiary lymphoid follicle formation, disruption of muscularis, smooth muscle cell loss, and other findings consistent with a pronounced tissue reaction. At and around the suture implantation site, there was moderate tissue injury, but the overlying mucosa was intact, with minimal-to-mild serosal neovascularization (Fig. 7).

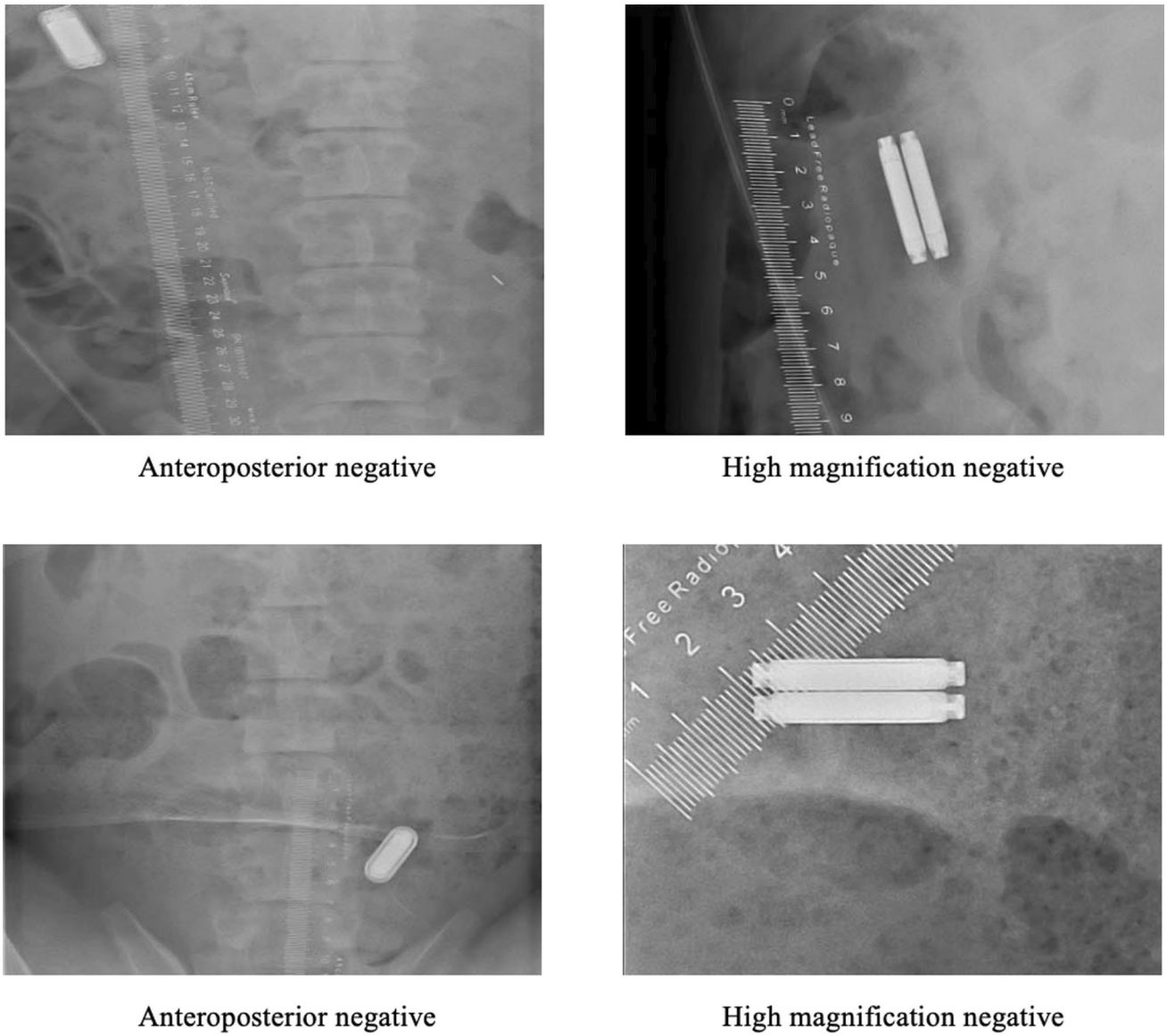

Fig. 3 Radiograph of magnetic compression anastomosis site in 4 animals, day of procedure

Discussion

In the development phase of the novel MCAD, 5 swine were treated with prototype devices of varying size to determine total dimensions of a linear magnet that would exert appropriate force to form a patent duodeno-ileal diversion anastomosis. In the verification study, an optimally sized magnet was inserted in 4 swine to confirm its ability to establish a magnetic DI as an antecedent to its use in human clinical trials. The MCAD proved safe and effective in creating a smooth and patent delayed compression anastomosis in the swine. At 6 weeks post procedure, all anastomoses had good healing with little inflammation or tissue reaction and new vascularization when compared to enterotomy sites.

Creation of a GI anastomosis is a critical feature of most MBS procedures upon which successful treatment depends. Suturing and stapling whether by hand, laparoscopy, endoscopy, or robot, are the current basis for accomplishing an anastomosis, although magnetic compression technique may offer an equally safe and effective, or better, alternative. Patients are inclined toward shorter, minimally invasive procedures that reduce operative risk and severe postoperative complications including anastomotic leak, bleeding, and stricture. Catastrophic anastomotic events may be averted by replacing suturing and stapling with proven magnetic compression devices.

Effective anastomoses formed by any method must be well vascularized, hemostatic, air-tight throughout their

Table 1 Animal weight over time

Day	Animal no				Min (kg)	Max (kg)	Mean (kg)
	Weight (kg)						
D0	54.4	53.8	56.7	59.1	53.8	59.1	56.0
D2	53.3	–	–	–	53.3	53.3	53.3
D3	52.7	54.5	57.4	60.3	52.7	60.3	56.2
D5	52.4	54.7	58.6	60.6	52.4	60.6	56.6
D8	52.5	54.1	57.9	60.7	52.5	60.7	56.3
D10	53.8	54.9	58.0	61.4	53.8	61.4	57.0
D12	51.9	55.3	58.5	62.2	51.9	62.2	56.5
D15	52.4	56.1	59.8	63.0	52.4	63.0	57.8
D17	53.8	57.7	60.0	63.3	53.8	63.3	58.7
D19	54.5	60.1	62.2	–	54.5	62.2	58.9
D22	54.9	61.6	60.7	–	54.9	61.6	59.1
D24	56.7	63.1	61.5	66.7	56.7	66.7	62.0
D26	–	–	–	67.9	67.9	67.9	67.9
D29	56.4	–	62.7	68.7	56.4	68.7	62.6
D31	57.1	65.8	61.9	69.7	57.1	69.7	63.6
D33	–	64.5	–	–	64.5	64.5	64.5
D36	62.3	64.5	69.3	74.4	62.3	4.4	67.6
D38	–	–	–	72.3	72.3	72.3	72.3
D39	58.3	64.5	68.5	70.5	58.3	70.5	65.5
Weight variation (kg))	3.9	10.7	11.8	11.4	3.9	11.8	9.5

– Not applicable

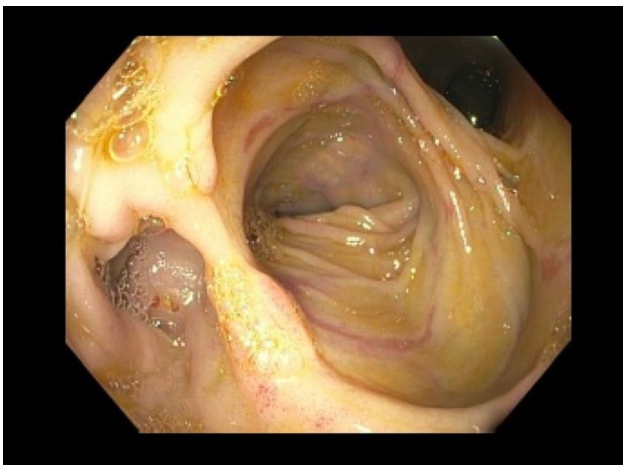

Fig. 4 A patent porcine duodeno-ileostomy at 6 weeks, on the right the double lumen afferent and efferent ileal loop, and on the left the native duodenum. In duodenoscopy of the pig, the endoscope must rotate 360° in the stomach, inversing the image

circumference, absent active disease, and tension free at their proximal and distal margins [19]. In our study, anastomoses formed by the MCAD in all 8 animals met these requirements at study endpoint while also retaining no foreign bodies that might incite inflammatory or fibrotic processes acutely or over time.

Observations from the current study agreed with prior studies that found formation of anastomoses by compression as effective as those by conventional methods. Summarizing CA technologies before 2008, Kaidar-Person et al. found CA technique a worthy alternative to conventional anastomosis formation by the outcome measures of safety, efficacy, and expense [19]. Diaz et al.'s 2019 review critically considered recent MCA technologies, concluding that the approach provides a safe, feasible means of GI anastomosis creation although individual device limitations require further research (e.g., rapid vs delayed anastomosis; potential leaks after blind magnet insertion; appropriate anastomosis sizing in diverse GI locations; interference with non-magnetic instruments) [40].

Preclinical studies of MCA technologies have mainly evaluated rodents, rabbits, and dogs [25–27, 41]. The current study focused on the large-animal subject most anatomically similar to humans. Other recent porcine studies include Wall et al.'s use of the magnamosis system in which 16 swine underwent magnetic side-to-side (SSA) or conventional end-to-side (ESA) colorectal anastomoses with hybrid natural orifice translumenal endoscopic surgery (NOTES) technique. They found inflammation and fibrosis similar between magnetic SSA and conventional stapled anastomoses at 10 days [23]; whereas, in the current study, tissue damage was apparent only in sutured enterotomy sites.

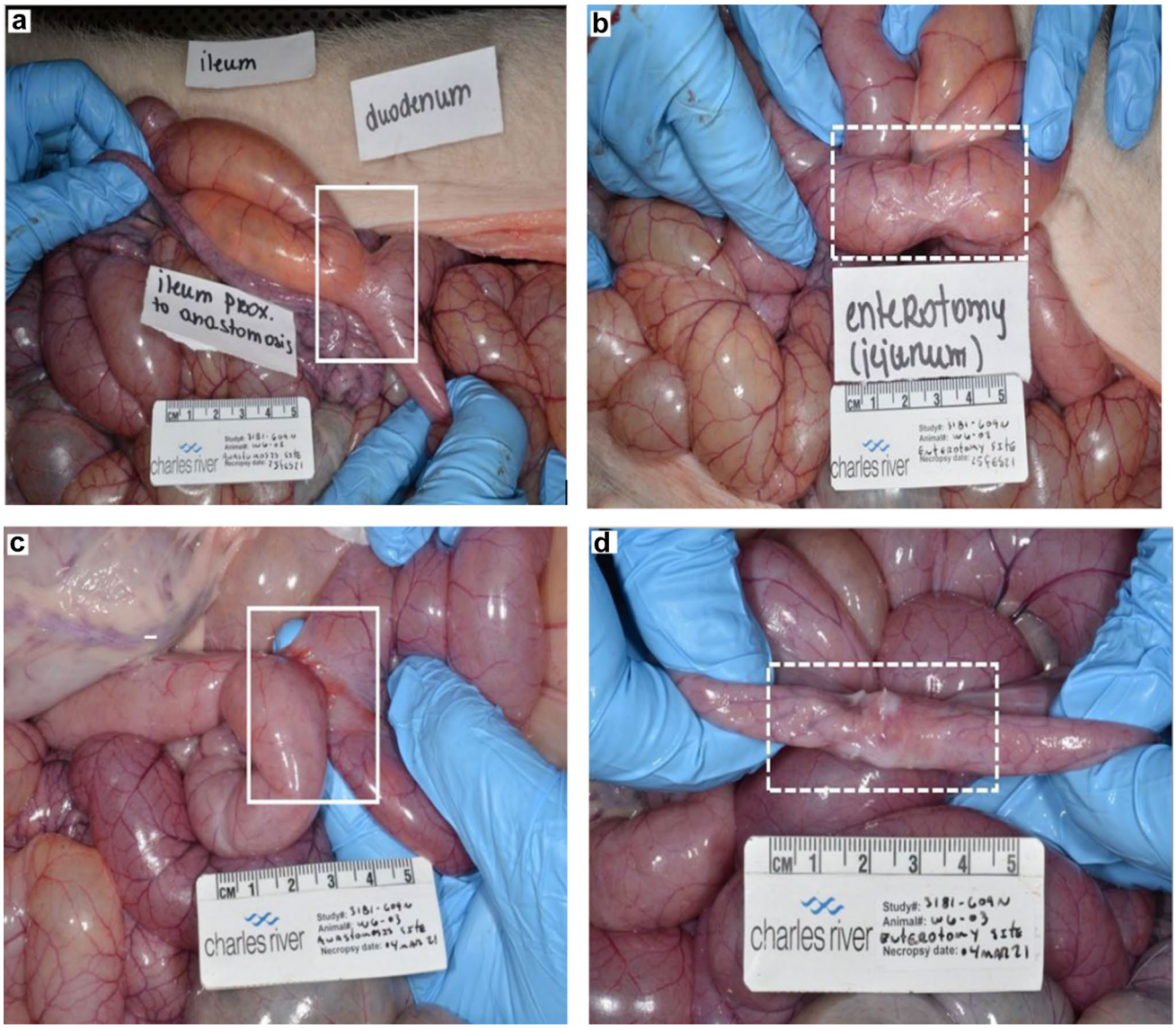

Fig. 5 Representative gross necropsy images of side-to-side duodeno-ileal (DI) magnetic compression anastomosis (MCA) and jejunal enterotomy (JE) sites. **a** Low magnification image of the serosal aspect of the side-to-side DI MCA site (white solid rectangle); **b** Low magnification image of the serosal aspect of the JE site (white dashed rectangle); **c** Higher magnification of the serosal aspect of the side-to-side DI MCA (white rectangle); **d** Higher magnification view of the serosal aspect of the JE site (dashed, white rectangle)

Ryou et al. studied a magnetic incisionless anastomosis system (IAS) to create a large-caliber anastomosis in 5 intervention and 3 control pigs. Intervention pigs underwent simultaneous enteroscopy and colonoscopy with 2 magnets deployed and mated under fluoroscopy; a jejunocolic anastomosis was created and the magnets gradually expelled. Study endpoints and outcomes were similar to those of the current study: in all pigs, the procedure was technically successful, anastomoses were patent, and histopathologic examination showed good epithelialization through the anastomosis without inflammation or fibrosis at 3 months. Significantly more weight loss was seen in intervention animals than controls consonant with the goals of MBS. Unlike the current study, the IAS technology required two endoscopists; in addition, some adjacent structures were inadvertently captured between the magnets [24]. In a later, related study, Ore et al. compared creation of an end-to-end small-bowel anastomosis after ileostomy takedown using self-forming magnets (SFMs, an evolution of the IAS) in 6 pigs to those of 4 stapled and 4 hand-sewn controls. The range of time to magnet expulsion was similar to that of the current study, as were histopathologic outcomes [28]. Several first-in-human studies of GI MCA have been completed. These address bowel obstruction, or aim to meet MBS objectives. In these studies of adult patients with follow-up of 6–34 months there were few anastomotic complications [29, 30, 32].

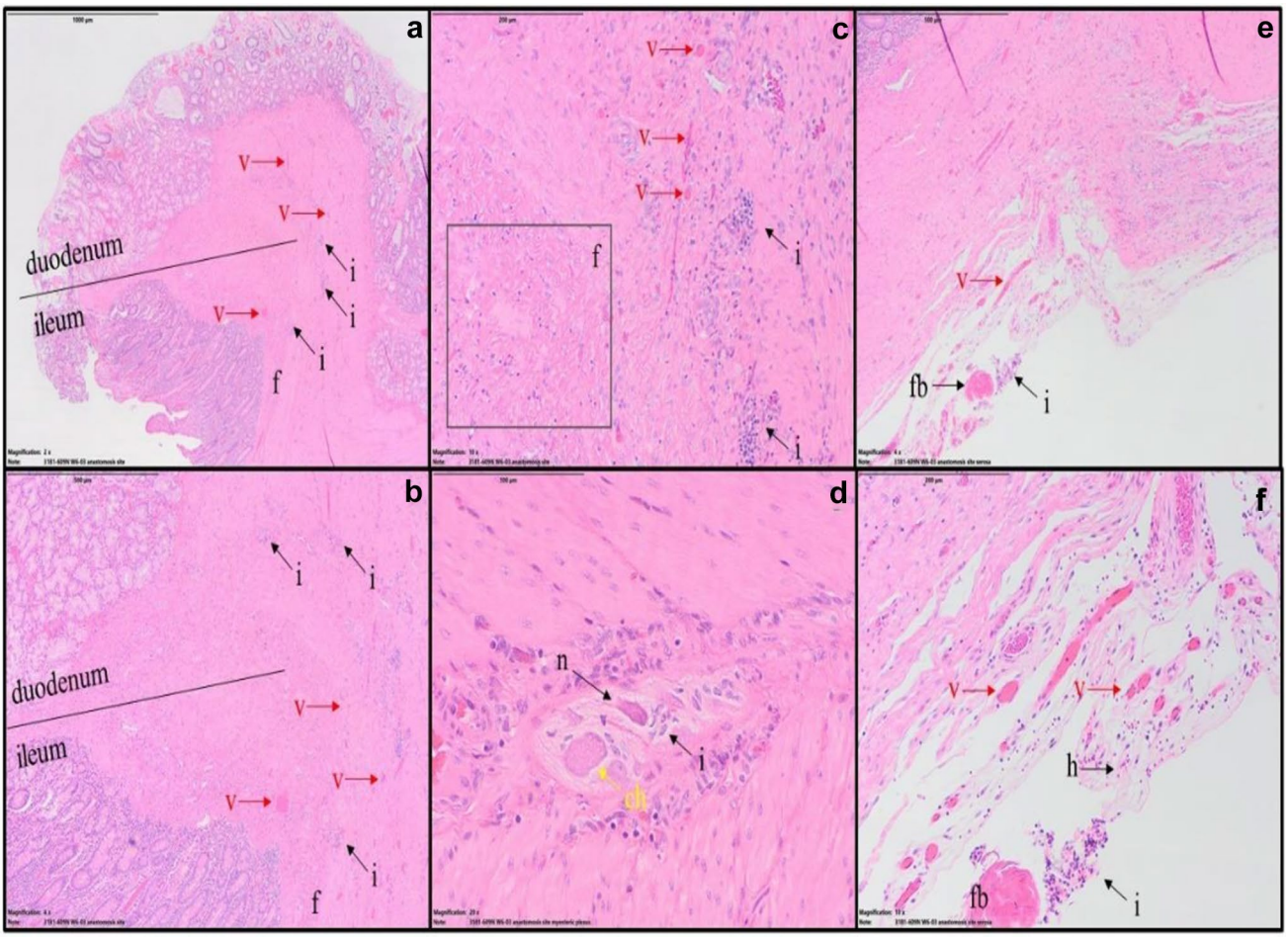

Fig. 6 Duodeno-ileal (DI) magnetic compression anastomosis (MCA) sites. H&E, DI site, 2X (**a**), 4X (**b**, **e**), 10X (**c**, **f**) and 20X (**d**). **a** The MCA site was characterized by minimal, multifocal, predominantly lymphocytic inflammation confined to the muscularis (black arrows, i) and well as neovascularization within the muscularis (red arrows, v). In addition, there was a focally extensive, minimal area of fibrosis within the muscularis at the MCA site, which infiltrated the smooth muscle (**f**). **b** Higher magnification of (**a**). **c** Detail of the muscularis at the DI site. The muscularis is characterized by a focally extensive area of fibrosis (black rectangle, f), neovascularization (red arrows, v) and multifocal aggregates of lymphocytes (black arrows, i). **d** Within the muscularis, at and adjacent to the MCA site, the myenteric plexi were hypercellular and infiltrated by small numbers of histocytes (black arrow, i). The neurons were characterized by necrosis (back arrow, n) or chromatolysis (yellow arrow, ch). **e** The serosal surface at the MCA site was characterized by minimal mesothelial hyperplasia and fibrosis with neovascularization (red arrow, v). Multifocally, within the hyperplastic mesothelium, there were entrapped foci of inflammatory cells, predominantly neutrophils (black arrow, i) and fibrin aggregates (black arrow, fb). **f** Higher magnification of (**e**). In addition to changes described in (**e**), within the serosal, hyperplastic mesothelial tissue there were minimal foci of hemorrhage (black arrow, h)

In the current investigation, with respect to safety, the swine that died from an internal hernia on POD 4 in the developmental phase emphasizes the importance of closure of mesenteric defects to avoid bowel entrapment. However, while these defects can be treated readily with standard surgical techniques in humans in a primary procedure [42], the approach is impractical in young swine as their intestinal mesentery is more diaphanous and sustains hemorrhage and hematoma with attempted suturing. In the verification study, the instance of internal hernia in one pig was successfully repaired by corrective surgery.

MBS studies of anastomosis creation by sewing or surgical stapling have substantially demonstrated that weight loss and co-existing medical conditions are dramatically improved. Our study assessed whether outcomes with the MCAD technology in large animals demonstrated an effective technology suitable for transfer to human study.

Limitations of this study include the use of pigs that were not obese. Although our choice of young, non-atherogenic pigs was intended to provide a model anatomically closest to humans, the swine model might have been one more commonly used in preclinical MBS studies to emulate

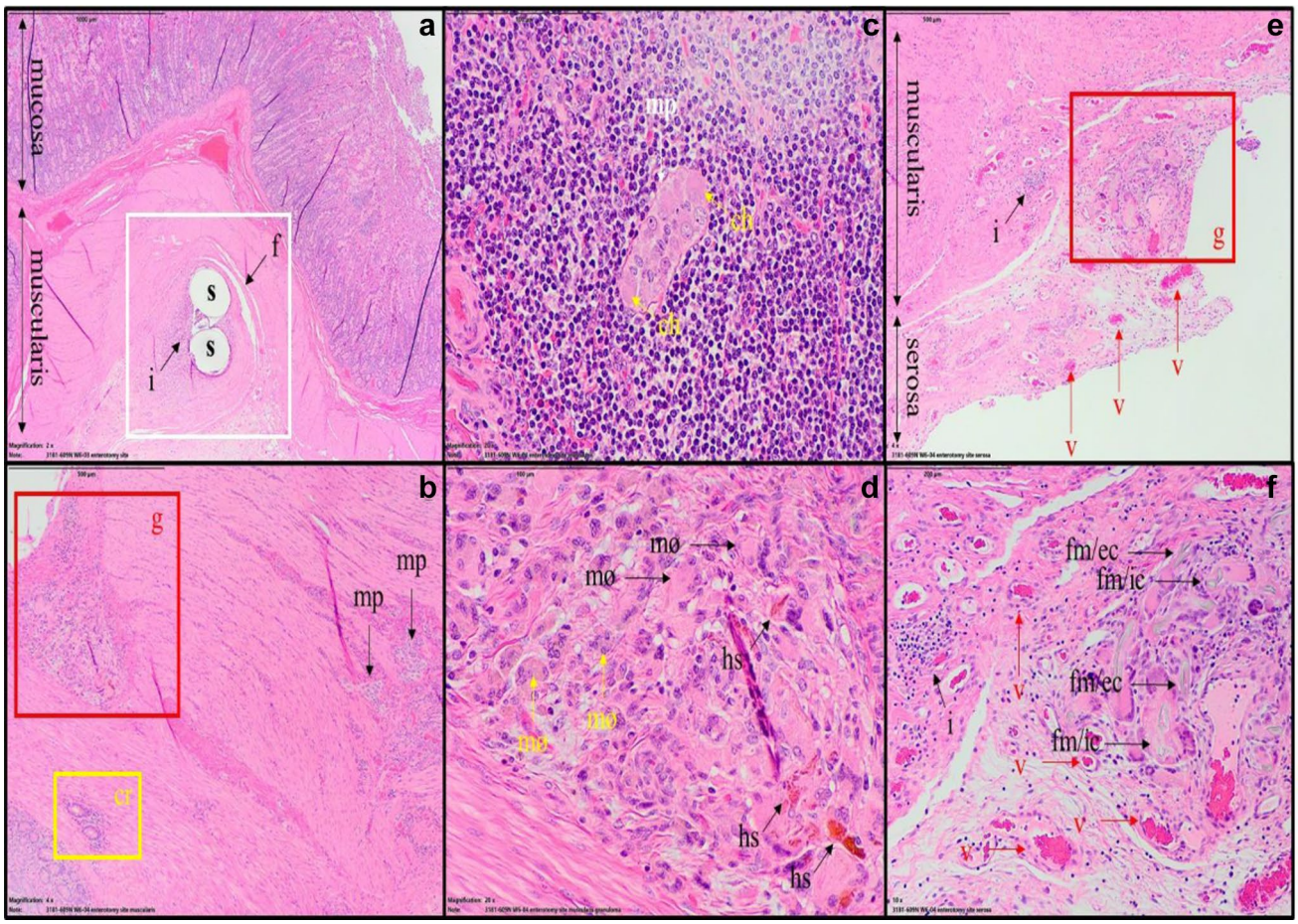

Fig. 7 Jejunal enterotomy (JE) sites. H&E, JE site, 2 X (**a**), 4X (**b**, **e**), 10X (**f**), and 20X (**c**, **d**). **a** Low magnification of the suture implantation site within the muscularis of the jejunum. The suture implantation site (white rectangle, s) was characterized by moderate mixed inflammatory infiltrate (black arrow, i) as well as minimal fibrosis encapsulating the suture material (black arrow, f). Overlying mucosa was intact. **b** Higher magnification view of the changes in the muscularis associated with the suture implantation site. Occasionally, within the muscularis at or adjacent to the implantation site there were granulomas (red square, g) or crypt herniation (yellow rectangle, cr). Changes in myenteric plexi such as chromatolysis, necrosis or histiocytic infiltration were also noted (black arrows, mp). **c** Within the muscularis at the JE site there was a tertiary lymphoid follicle associated with suture implantation that encircled the myenteric plexus (white arrow, mp) that displayed prominent neuronal chromatolysis (yellow arrows, ch). **d** Higher magnification of area in (**b**) highlighted by a red square. Granuloma within the muscularis associated with the suture implantation site was composed of macrophages (mø, black arrows), some of which contained dark brown particulate intracytoplasmic material (mø, yellow arrows). Within the granuloma, there was accumulation of extracellular, brown material interpreted as hemosiderin (black arrows, hs). **e** Low magnification view of the serosa at the JE site. Serosa is characterized by mild serosal fibrosis/mesothelial hyperplasia and the resultant tissue is well vascularized (red arrows, v). At the junction with the muscularis, the fibrous connective tissue is expanded by a focal granuloma (red rectangle, g). Adjacent muscularis contains multifocal predominantly lymphocytic inflammatory aggregates (black arrow, i). **f** Higher magnification of (**e**). Granuloma at the junction between hyperplastic serosa and the muscularis was predominantly composed of macrophages and multinucleated giant cells. Granuloma contained non-birefringent foreign material, interpreted as suture material, which was extracellular (black arrows, fm/ec) or intracellular and located within the cytoplasm of multinucleated giant cells (black arrows, fm/ic). Surrounding serosa was well vascularized (red arrows, v). Adjacent muscularis also had foci of neovascularization (red arrow, v) and contained multifocal aggregates of mixed inflammatory cells (black arrow, i)

postoperative human physiologic changes. In comparison to the human intestinal tract, the small bowel walls of swine are thinner, the length is markedly longer (20 m vs ≤ 7 m), and their diameter is 1.0–1.5 cm vs 2.5–4.0 cm; in spite of the smaller diameter and longer passageway, all magnets positioned in the pigs passed freely. Other limitations were the small sample and the absence of a control group.

Conclusions

Insertion of a novel MCA device to gradually form a patent duodeno-ileostomy was technically straightforward and proved safe and effective in a porcine model. At 6 weeks post procedure, magnetically created anastomoses exhibited excellent healing characterized by low levels of

inflammation, minimal tissue reaction, and good vascularization compared to sutured enterotomy sites. This preclinical study suggests the feasibility of using the novel magnetic compression anastomosis device in humans.

Acknowledgements The authors thank the Charles River Laboratories staff for their excellent conduct of the veterinary study, in particular, Aurelia Spataru-Burgoci, Rosa Kaviani, and Joanna M. Rybicka.

Funding This study was supported by a research grant from GT Metabolic Solutions (San Jose, CA). Michel Gagner is a consultant with stock options in GT Metabolic Solutions. Michel Gagner is also a consultant for Medtronic, Inc. and Lexington Medical, Inc. and has stock options in Lexington Medical, Inc. Todd Krinke is an employee with stock options in GT. Maxime LaPointe-Gagner is employed by Westmount Surgical Center and has no conflicts of interest or financial ties to pharmaceutical or device companies to disclose. Jane Buchwald is a GT consultant with GT stock options; she received grants from Ethicon, Inc., M.I.D., Society of Bariatric and Metabolic Surgeons of Kazakhstan, Medical Faculty of Mannheim, Holy Family Hospital, Israel, and the American College of Surgeons.

Declarations

Ethical approval All procedures of the study were conducted in compliance with the protocol and the standard operating procedures and institutional review board of the testing facility, Charles River Laboratories (Boisbriand, Quebec, Canada).

Human and animal rights The study was performed in accord with the ethical standards of the animal testing facility's Institutional Animal Care and Use Committee (IACUC) to ensure compliance with the Canadian Council on Animal Care regulations and National Academies of Science Guide for Care and Use of Laboratory Animals. No written consent was needed for an animal study.

References

1. Kirwan JP, Courcoulas AP, Cummings DE, Goldfine AB, Kashyap SR, Simonson DC et al (2022) Diabetes remission in the Alliance of Randomized Trials of Medicine Versus Metabolic Surgery in Type 2 Diabetes (ARMMS-T2D). Diabetes Care 45(7):1574–1583
2. Sarwer DB, Gasoyan H, Bauerle Bass S, Spitzer JC, Soans R, Rubin DJ (2021) Role of weight bias and patient-physician communication in the underutilization of bariatric surgery. Surg Obes Relat Dis 17(11):1926–1932
3. Amat C (1895) Appareils a sutures: les viroles de denans; les points de Bonnier; les boutons de Murphy. Arch Med Pharmacie Militaires Paris 25:273–285
4. Murphy JB (1892) Cholecysto-intestinal, gastro-intestinal, entero-intestinal anastomosis, and approximation without sutures. Med Rec N Y 42:665–676
5. Mayo WJ, Mayo CH (1895) Clinical report—I: Complete section of the vas deferens, end-to-end union; II: acute suppuration of knee-joint: open treatment; III: gastro-enterostomy by the murphy button: anastomoses by this method. Ann Surg 21(1):35–44
6. Stewart D, Hunt S, Pierce R, Dongli M, Frisella M, Cook K et al (2007) Validation of the NITI endoluminal compression anastomosis ring (EndoCAR) device and comparison to the traditional circular stapled colorectal anastomosis in a porcine model. Surg Innov 14(4):252–260
7. Tucker ON, Beglaibter N, Rosenthal RJ (2008) Compression anastomosis for Roux-en-Y gastric bypass: observations in a large animal model. Surg Obes Relat Dis 4(2):115–121
8. Gagner M, Heppell J, Lamarre L, Carioto S (1993) L'anastomose colique par laparoscopie avec l'anneau biodégradable valtrac: Une étude comparative dans un modèle canin. Ann Chir 46(9):875
9. Kanshin NN, Lytkin MI, Knysh VI, lu Klur V, Khamidov AI, (1984) First experience with application of compression anastomoses with the apparatus AKA-2 in operations on the large intestine. Vestn Khir Im I I Grek 132:52–57
10. Hardy TG, Aguilar PS, Stewart WR, Katz AR, Maney JW, Costanzo JT et al (1987) Initial clinical experience with a biofragmentable ring for sutureless bowel anastomosis. Dis Colon Rectum 30(1):55–61
11. Rebuffat C, Rosati R, Montorsi M, Fumagalli U, Maciocco M, Poccobelli M et al (1990) Clinical application of a new compression anastomotic device for colorectal surgery. Am J Surg 159:330–335
12. Bubrick MP, Corman ML, Cahill CJ, Hardy TG, Nance FC, Shatney CH (1991) Prospective, randomized trial of the biofragmentable anastomosis ring. Invest Group Am J Surg 161:136–142
13. Cossu ML, Coppola M, Fais E, Ruggiu M, Spartà C, Profili S et al (2000) The use of the Valtrac ring in the upper and lower gastrointestinal tract, for single, double, and triple anastomoses: a report of 50 cases. Am Surg 66(8):759–762
14. Nudelman IL, Fuko V, Greif F, Lelchuk S (2002) Colonic anastomosis with the nickel-titanium temperature-dependent memory-shape device. Am J Surg 183:697–701
15. Lee JY, Woo JH, Choi HJ, Park KJ, Roh YH, Kim KH, Lee HY (2011) Early experience of the compression anastomosis ring (CAR™ 27) in left-sided colon resection. World J Gastroenterol 17(43):4787–4792
16. Ye F, Chen D, Wang D, Lin J, Zheng S (2014) Use of Valtrac™-secured intracolonic bypass in laparoscopic rectal cancer resection. Medicine (Baltimore) 93(29):e224
17. Bobkiewicz A, Studniarek A, Krokowicz L, Szmyt K, Borejsza-Wysocki M, Szmeja J et al (2017) Gastrointestinal tract anastomoses with the biofragmentable anastomosis ring: is it still a valid technique for bowel anastomosis? Analysis of 203 cases and review of the literature. Int J Colorectal Dis 32(1):107–111
18. Gagner M (2021) Laparoendoscopic magnetic gastrointestinal anastomosis. In: Gagner M (ed) Magnetic surgery. Springer Publisher, New York, pp 135–148
19. Kaidar-Person O, Rosenthal RJ, Wexner SD, Szomstein S, Person B (2008) Compression anastomosis: history and clinical considerations. Am J Surg 195:818–826
20. Marrache MK, Itani MI, Farha J, Fayad L, Sharara SL, Kalloo AN et al (2021) Endoscopic gastrointestinal anastomosis: a review of established techniques. Gastrointest Endosc 93(1):34–46
21. Jamshidi R, Stephenson JT, Clay JG, Pichakron KO, Harrison MR (2009) Magnamosis: magnetic compression anastomosis with comparison to suture and staple techniques. J Pediatr Surg 44(1):222–228
22. Ryou M, Cantillon-Murphy P, Azagury D, Shaikh SN, Ha G, Greenwalt I et al (2011) Smart self-assembling magnets for endoscopy (SAMSEN) for transoral endoscopic creation of immediate gastrojejunostomy (with video). Gastrointest Endosc 73(2):353–359
23. Wall J, Diana M, Leroy J, Deruijter V, Gonzales KD, Lindner V et al (2013) MAGNAMOSIS IV: magnetic compression anastomosis for minimally invasive colorectal surgery. Endoscopy 45(8):643–648
24. Ryou M, Agoston AT, Thompson CC (2016) Endoscopic intestinal bypass creation by using self-assembling magnets in a porcine model. Gastrointest Endosc 83(4):821–825

25. Zhao G, Ma J, Yan X, Li J, Ma F, Wang H et al (2019) Optimized force range of magnetic compression anastomosis in dog intestinal tissue. J Pediatr Surg 54(10):2166–2171
26. Chen H, Ma T, Wang Y, Zhu HY, Feng Z, Wu RQ et al (2020) Fedora-type magnetic compression anastomosis device for intestinal anastomosis. World J Gastroenterol 26(42):6614–6625
27. Zhang M, Lyu X, Zhao G, An Y, Lyu Y, Yan X (2022) Establishment of Yan-Zhang's staging of digestive tract magnetic compression anastomosis in a rat model. Sci Rep 12:12445
28. Ore AS, Askenasy E, Ryou M, Baldwin T, Thompson CC, Messaris E (2022) Evaluation of sutureless anastomosis after ileostomy takedown using the self-forming magnet anastomosis system in a porcine model. Surg Endosc 36(10):7664–7672
29. Graves CE, Co C, Hsi RS, Kwiat D, Imamura-Ching J, Harrison MR, Stoller ML (2017) Magnetic compression anastomosis (magnamosis): first-in-human trial. J Am Coll Surg 225:676–681
30. Kamada T, Ohdaira H, Takeuchi H, Takahashi J, Ito E, Suzuki N et al (2021) (2021) New technique for magnetic compression anastomosis without incision for gastrointestinal obstruction. J Am Coll Surg 232(2):170-177.e2
31. van Hooft JE, Vleggaar FP, Le Moine O, Bizzotto A, Voermans RP, Costamagna G et al (2010) Endoscopic magnetic gastroenteric anastomosis for palliation of malignant gastric outlet obstruction: a prospective multicenter study. Gastrointest Endosc 72:530–535
32. Schlottmann F, Ryou M, Lautz D, Thompson CC, Buxhoeveden R (2021) Sutureless duodeno-ileal anastomosis with self-assembling magnets: safety and feasibility of a novel metabolic procedure. Obes Surg 31(9):4195–4202
33. Gagner M (2021) Introduction: ideas and people leading to successful products for patient care leading to magnetic surgery: Chapter 1. In: Gagner M (ed) magnetic surgery. Springer Publisher, New York, pp 1–6
34. Gruenberger JM, Karcz-Socha I, Marjanovic G, Kuesters S, Zwirska-Korczala K, Schmidt K, Karcz WK (2014) Pylorus preserving duodeno-enterostomy with sleeve gastrectomy – preliminary results. BMC Surg 14:20–28
35. National Academy of Sciences (2011) Guide for the care and use of laboratory animals, 8th edn. The National Academies Press, Washington
36. Gagner M (2009) Emerging techniques in bariatric surgery—laparoscopic duodeno-ileostomy. ACS-2771 Online video Library of the American College of Surgeons
37. Gagner M (2015) Safety and efficacy of a side-to-side duodeno-ileal anastomosis for weight loss and type-2 diabetes: duodenal bipartition, a novel metabolic surgery procedure. Ann Surg Innov Res 14(9):6
38. Edwards MA, Jones DB, Ellsmere J, Grinbaum R, Schneider BE (2007) Anastomotic leak following antecolic versus retrocolic laparoscopic Roux-en-Y gastric bypass for morbid obesity. Obes Surg 17:292–297
39. Lim R, Beekley A, Johnson DC, Davis KA (2018) Early and late complications of bariatric operation. Trauma Surg Acute Care Open 3(1):e000219
40. Diaz R, Davalos G, Welsh LK, Portenier D, Guerron AD (2019) Use of magnets in gastrointestinal surgery. Surg Endosc 33(6):1721–1730
41. Qiao W, Shi A, Ma F, Yan X, Duan J, Wu R et al (2020) Further development of magnetic compression for gastrojejunostomy in rabbits. J Surg Res 245:249–256
42. Comeau E, Gagner M, Inabnet WB, Herron DM, Quinn TM, Pomp A (2005) Symptomatic internal hernias after laparoscopic bariatric surgery. Surg Endosc 19(1):34–39